A Smart Environment-Adapting Timed-Up-and-Go System Powered by Sensor-Embedded Insoles

Zhuolin Yang, *Student Member, IEEE*, Chen Song, *Student Member, IEEE*, Feng Lin, *Member, IEEE*, Jeanne Langan, *Member, IEEE*, and Wenyao Xu, *Member, IEEE*

***Abstract*—With the growth of the elder population, fall risk evaluation is crucial to prevent elders from serious injuries, as well as reduce related financial burdens. A balance assessment, timed up and go (TUG), has been widely used to estimate fall risk. The standardized TUG focuses on flat ground walking with no environmental variance. Therefore, it falls short of assessing an individual's gait adaptability. Being able to adjust steps in response to environmental changes, for example, needing to navigate around or over a child's toy left on the sidewalk, is essential to avoid fall risk and fundamental to community ambulation. To this end, we propose four environment-adapting TUGs designed to assess one's ability to adapt gait in complex environments and a compatible system named Smart Insole TUG (SITUG), which provides real-time, feature-rich, and ease-of-operation TUG analysis. Based on experimental results, SITUG is capable of extracting gait related spatial–temporal features with all mean accuracies over 92%. Besides, the system achieves a mean accuracy of 92.23% in segmenting *five* TUG phases.**

***Index Terms*—Gait analysis, sensors, signal processing, wearable computers.**

I. Introduction

ACCORDING to an aging statistics [1], the older population is tremendously expanding; approximately 98 million elders will live in the U.S. by the year 2060. With this ongoing growth, the older population's health condition increasingly draws attention. Falls are the leading cause of injury and fatality among older adults. An older adult receives emergency services every 11 s due to a fall. Furthermore, there is a death every 19 min due to a fall [2]. Financial burdens associated with falls are oppressive as well. The total cost of fall injuries was $34 billion in 2013 and the cost is trending upward [2].

Timed up and go (TUG) is recommended by the American Geriatric Society and the British Geriatric Society [3] and has been widely applied for gait and fall risk assessment. However, the standardized TUG analysis simply relies on the amount of time to complete test procedure and ignores the value of kinematic data. As criticized by studies [4]–[7], the standardized assessment is not comprehensive enough to fully evaluate an individual's risk of falling. For improving the deficiency, novel measurements of TUG deploy technological devices for collections of detailed test data and significantly increase the reliability of fall risk estimation [7]. Nevertheless, further advancements are still needed due to their inconveniences. Most of the technology-based TUG measurements require multiple sensor attachments on each testee's body or bulky devices (e.g., cameras and tablets) nearby [7]–[9]. In addition, many of them are incapable of providing feature-rich and real-time TUG test results.

Apart from the insufficiency or the inconveniences of standardized and technology-based TUG measurements, another justifiable concern about TUG is that it only involves movements on a clean and flat platform with severely limited environmental variances. Thus, it is incapable of testing gait adaptability, the ability to adjust gait in response to environmental changes [10], which is strongly related to fall risk [11], [12]. External, situational factors (e.g., obstacles and inclines) can be effective in provoking, testing gait adaptability [10], and promoting fall risk analysis [12], [13]. Despite the drawback of TUG (i.e., no external factor), virtues are worth preserving. For instance, TUG procedure involves representative movements (e.g., stand up, walk, turn, and sit down) in our daily life requiring no complex instruction. Therefore, we invented four environment-adapting TUGs involving an extended distance, an incline, or obstacles (see Section II-C). Clearly, an unobtrusive system is of great importance for assessing TUG with external factors.

To this end, we introduce a feature-rich, real-time, and ease-of-use system for assessing TUG with or without obstacles and inclines. Our system, Smart Insole TUG (SITUG), enhances TUG measurements by facilitating data collection and augmenting data analysis. The system is built based on a sensor-equipped insole, a smartphone application, and a cloud service module. It is capable of extracting rich gait features, offering advanced information about an individual's mobility. Based on these features, SITUG provides further information

Manuscript received February 27, 2018; revised April 28, 2018; accepted May 27, 2018. Date of publication June 7, 2018; date of current version May 8, 2019. This work was supported in part by the U.S. National Institute of Health under Grant 01R21EB024731 and in part by the Pilot Project Research Training Program of the NY and NJ Education and Research Center, National Institute for Occupational Safety and Health under Grant T42-OH-008422. *(Corresponding author: Wenyao Xu.)*

Z. Yang, C. Song, and W. Xu are with the Department of Computer Science and Engineering, State University of New York at Buffalo, Buffalo, NY 14260 USA (e-mail: zhuoliny@buffalo.edu; csong5@buffalo.edu; wenyaoxu@buffalo.edu).

F. Lin was with the Department of Computer Science and Engineering, State University of New York at Buffalo, Buffalo, NY 14260 USA. He is now with the Department of Computer Science and Engineering, University of Colorado Denver, Denver, CO 80204 USA (e-mail: feng.2.lin@ucdenver.edu).

J. Langan is with the Department of Rehabilitation Science, State University of New York at Buffalo, Buffalo, NY 14260 USA (e-mail: jlangan@buffalo.edu).

Digital Object Identifier 10.1109/JIOT.2018.2844837

related to falls by distinguishing five phases of TUG process. Compared to an earlier version of SITUG [14], this paper presents a more adaptive and mature system in terms of gait analysis and TUG segmentation (see Section IV).

II. Preliminaries

A. Timed Up and Go

TUG is a well known screening test used in fall risk analysis. It consists of fundamental, representative daily life movements requiring no lengthy instruction and training. In a regular TUG procedure, the subject is asked to get up from a chair, walk a 3-m distance on the flat ground at a comfortable pace, turn around, walk back to the chair, and then sit back down [7]. Nevertheless, TUG and its standardized measurement can be insufficient for comprehensive fall risk estimation. The standardized determination of high fall risk is based on the total time to complete the procedure; a subject's kinematic data are not recognized leading to lost information in mobility and balance analyses [4]. Moreover, TUG involves only flat ground walking with no environmental variance. It is reasonable to criticize the capability of TUG in assessing an individual's ability to perform suitable gait patterns for coping with environmental variances, i.e., gait adaptability [10], which significantly contributes to falls [11], [12]. Overall, it is demanded to analyze TUG from an in-depth perspective with meaningful quantitative features and considerations of gait adaptability.

B. Sensor-Based TUG Analysis

Sensor-based TUG analysis is developed for providing useful kinematic data. By deploying camera and inertial measurement units (IMUs), novel TUG analysis systems are able to extract meaningful gait and TUG features. In some camera-based measurement studies [15], [16], the total taken steps and the duration of some test phases (e.g., turning and sitting down) are extracted automatically via video filming. Knowing the time taken in different TUG phases improves the reliability of estimating fall risk [7]. However, the camera-based methods have obvious drawbacks in practical usages. The camera setup is crucial. The position of cameras and the lighting of environments must be carefully adjusted. Moreover, they cannot monitor and assess in-depth kinematic data, like a detailed orientation of foot, which can be described as pitch, roll, and yaw angles.

IMU-based measurement systems utilize an electronic device which contains accelerometers, gyroscopes and more, offering linear accelerations and angular velocities of movements. These systems provide representative data of gait (e.g., stride count and stride length) and detailed information of TUG process (e.g., turn time and walk time) [7]. However, they require either clumsy sensor attachments or bulky devices. For instance, a reliable instrumented system, named iTUG [8], needs seven sensor attachments over the human body. Another well-developed system, QTUG [9], depends on two sensors and deploys an inconvenient tablet rather than a handy smartphone. Additionally, the data feedback of some systems is relatively tardy, like iTUG [8] which provides no real-time test report.

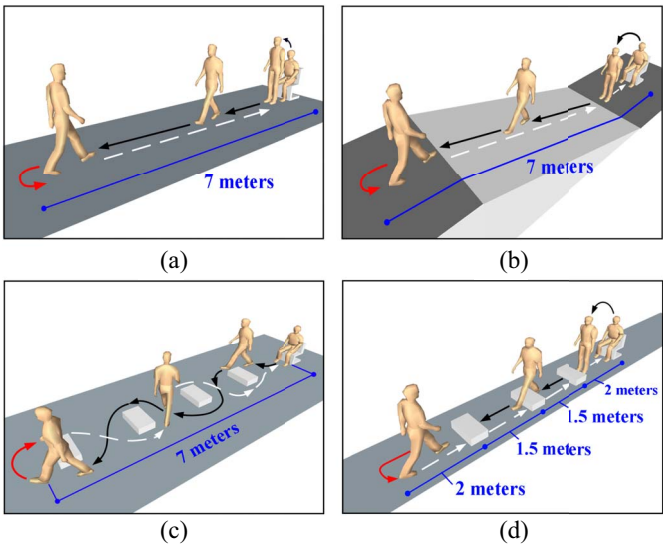

Fig. 1. Four environment-adapting TUG tests. (a) Extended TUG: standardized TUG with the extended distance. (b) Incline TUG: TUG with the incline factor. (c) Bypass TUG: TUG with the obstacle factor. Participants should go around obstacles. (d) Overpass TUG: participants should step over obstacles.

C. Environment-Adapting TUG

About 31% of falls in elders are accident and environment related [17]. Poor gait adaptability can contribute to falls under environmental variances (e.g., obstacles and inclines) placing elders at an increased danger [10], [11]. Studies have provoked and examined the gait adaptability by assessing obstacle or incline involved walking strategies [12], [18], [19], which can provide further fall risk related information. For examples, older adults with high fall risk demonstrate shorter step lengths and slower walking velocity compared to elders with low fall risk while walking on an incline [13]; in settings with obstacles, the aforementioned quantitative declines in step length and walking velocity are more distinct in older participants with higher fall risk compared to younger testees [19]. Overall, the gait adaptability can be elicited by involving obstacle, incline in walk producing informative fall risk related data. Consequently, we developed four environment-adapting TUGs to improve the standardized TUG setup with lack of induced gait adaptability, which are introduced as follows.

1) *Extended TUG:* The extended version of the standardized TUG. The distance between the chair and the turning point is 7 m as presented in Fig. 1(a).
2) *Incline TUG:* The walking should happen on an incline. Other activities (e.g., turning, standing up, and sitting down) are still performed on flat ground [see Fig. 1(b)].
3) *Bypass TUG:* Each subject should avoid four obstacles on flat ground by passing aside the obstacle [see Fig. 1(c)]. The displacement is 7 m and the estimated walking distance (WD) is 7.75 m from the chair to the turning point.

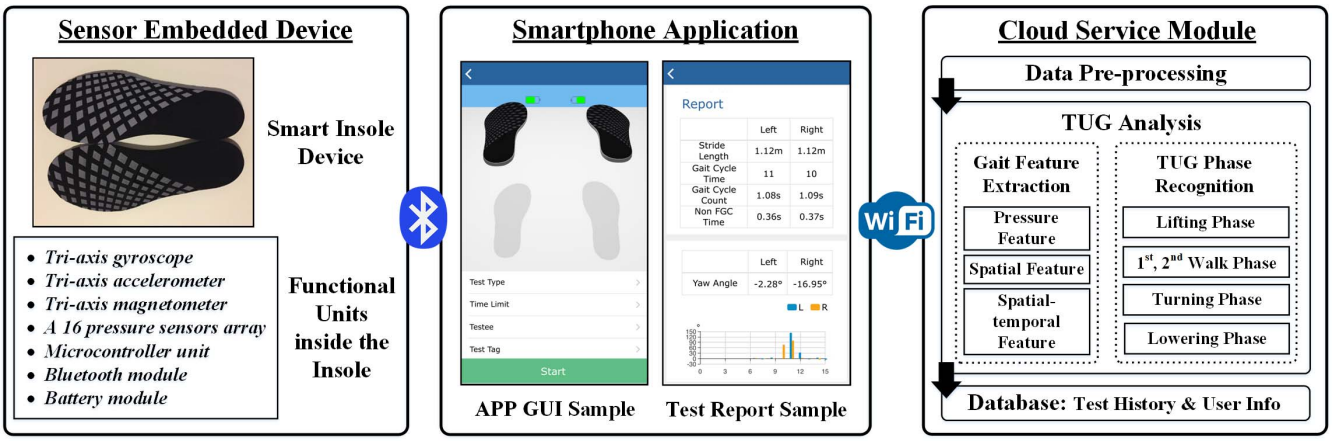

Fig. 2. Overall framework of our proposed system, SITUG. It contains a sensor embedded device, Smart Insole, a matched smartphone application, and a cloud service module. A photograph of the actual Smart Insole is presented under *sensor embedded device*. Pictures of the smartphone app are placed under *smartphone application*.

4) *Overpass TUG:* Details are shown in Fig. 1(d). Every subject avoids three obstacles on flat ground by stepping over the obstacle.

D. System Design Consideration

Current sensor-based TUG analysis systems are not convenient and comprehensive enough for environment-adapting TUGs since they require clumsy on-body sensors, nearby devices, or provide half-baked, dilatory data analyses. Under obstacle and incline involved situations, environmental-adapting TUGs demand a light and smooth system offering fine-grained data processing. After careful considerations, our system named SITUG should satisfy the following requirements.

1) *Unobtrusive:* No sensor attachment or camera setup.
2) *Comprehensive:* Well considered data analysis.
3) *Reliable:* High accuracy in gait and TUG data analysis.
4) *Robust:* No trouble with different walking environments.
5) *Real-Time:* Accessible real-time test results.

III. System Design

A. Design Overview

As shown in Fig. 2, our system is composed of a sensor embedded device, a smartphone application, and a cloud service module. The sensor embedded device, named Smart Insole, collects quantitative data such as angular velocities, linear accelerations, and pressures, during each test performance. The smartphone application is acting as a bridge between the Smart Insole and the cloud service module. Commanded by the application through Bluetooth, the insole collects and transfers raw data of each test. The application wirelessly receives and uploads the collected raw data to our cloud service module for operating the data preprocessing and the TUG analysis. At the end, a test report is sent to the smartphone application. Furthermore, our cloud service module can save physical information and test histories of each user. The followings are descriptions of different modules.

B. Smart Insole

Our wearable sensor embedded device is shown in Fig. 2 (left), *Smart Insole Device*. It has a similar hardware design to its previous version [20]. This insole integrates an IMU (i.e., a tri-axis gyroscope, a tri-axis accelerometer, and a tri-axis magnetometer) and a 16 pressure sensors array for data sensing. Specifically, IMU provides geometry features of gait and the pressure sensors array detects the plantar pressure distribution in walking which both significantly reflects gait abnormalities of an individual [21], [22]. Moreover, while the IMU is the most widely deployed sensor in gait analysis, the pressure sensors array can promote accuracy and efficiency in some aspects of gait analysis. For example, it can directly detect any foot-ground contacts (e.g., heel and toe strikes) because the pressure abruptly increases at the related plantar areas, while the IMU-based method indirectly indicates the contacts relying on the foot orientation information [23]. Besides from the data sensing accomplished by the two sensors, data acquisition is through the use of a 16 to 1 channel MUX and a Microcontroller Unit; data transferring is achieved via a Bluetooth low energy module. The insole also contains a battery module which is charged through USB connection. All the aforementioned components except the pressure sensors array are placed in a 40 mm by 40 mm printed circuit board.

C. Smartphone Application

We designed the smartphone application by prioritizing ease-of-operation considering most users are older adults who may have less experience with smartphone softwares compared to other age groups. The application connects the Smart Insole through Bluetooth so that users can choose when to collect data by simply clicking a button. The design of the smartphone application's graphical user interface is shown in Fig. 2 (middle). Our software automatically transfers data from the insole to the cloud service module for the data preprocessing and the TUG analysis via Wi-Fi or LTE. Moreover, a testee's physical information and test reports can be viewed inside the application. A sample of test report is presented in Fig. 2 (middle).

D. Cloud Service Module

The cloud service module is the core part in our system design. It has two main missions, the data preprocessing for limiting noises, drifts, and biases and the TUG analysis for

TABLE I
DESCRIPTIONS AND METHODOLOGIES OF PRESSURE FEATURES

Features	Methodology
Forefoot Average Pressure	The mean of $1^{th}-10^{th}$ pressure sensors' values.
Rearfoot Average Pressure	The mean of $11^{th}-16^{th}$ pressure sensors' values.
Sole Average Pressure	The mean of all pressure sensors' values.
(Fig. 3 (left) shows positions of $1^{th}-16^{th}$ pressure sensors in the insole.)	
Center of Pressure (COP) Location	P_i: the value of i^{th} pressure sensor. $n=16$: the total amount of pressure sensors. (X_i, Y_i): coordinate values of the i^{th} pressure sensor. (X_{cop}, Y_{cop}): the position of COP on the sole. $X_{cop}=(\sum_i^n X_i P_i)/(\sum_i^n P_i)$ $Y_{cop}=(\sum_i^n Y_i P_i)/(\sum_i^n P_i)$
Center of Pressure Velocity (V_{cop})	X_{dist}, Y_{dist}: COP travel distances on X-, Y-axes in a time interval $\triangle t$. $X_{dist}=\lvert X_{cop}(t+\triangle t)-X_{cop}(t)\rvert$ $Y_{dist}=\lvert Y_{cop}(t+\triangle t)-Y_{cop}(t)\rvert$ V_{cop}: the speed of COP location movements in a time interval $\triangle t$. $V_{cop}=(1)/(\triangle t)*\sqrt{(X_{dist})^2+(Y_{dist})^2}$

providing rich, robust, and real-time test results. The former includes: 1) denoising pressure values; 2) calibrating, filtering accelerometer and gyroscope data; and 3) initializing the baseline with magnetometer data [20]. The latter contains two analyses, gait feature extraction and TUG phase recognition. Three types of gait feature are extracted and five TUG phases are recognized, leading to an in-depth TUG gait analysis. In addition, the cloud service module includes a database function for storing test histories and user information. The structure of this module is presented in Fig. 2 (right) and all related methodologies are described in Section IV.

IV. COMPETENT TUG ANALYSIS

A. Gait Feature Extraction: Pressure Feature

All pressure features (see Table I) are derived from values given by a 16 pressure sensors array. Each pressure sensor is built based on a cutting-edge sensor technique, named electrical textile. The textile is coated with conductive polymer and air gapped at its inner structure. The initial resistance of textile is high and will decrease if its intra is squeezed by an applied force on the textile surface. Meanwhile, the output voltage, which can be transformed into pressure value, will increase. As shown in Table I, SITUG provides average pressures, center of pressure (COP) location, and COP velocity. While COP-based parameters are reliable measures of balance control [24], average pressure values in different plantar areas are essential for spatial–temporal feature extractions (see Section IV-C).

B. Gait Feature Extraction: Spatial Feature

Spatial features including pitch, roll, and yaw angles can be described as rotational angles around *x*-, *y*-, and *z*-axes of the insole in a world frame as shown in Fig. 3 (right). Introduced by Janota *et al.* [25], the quaternion-based algorithm is superior compared to anther two widely used methods, the rotational matrix transformation and the rotational angle rate integration, due to its efficiency and accuracy. A fast version of quaternion-based algorithm for deriving these angles are used in SITUG since it achieves the same accuracy as

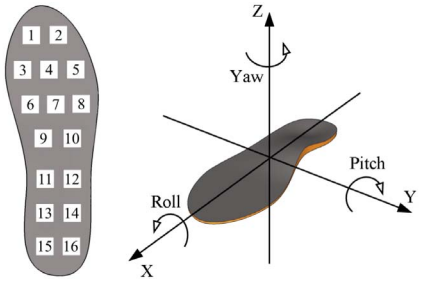

Fig. 3. Left: position of a 16 pressure sensors array in the insole. Right: roll, pitch, and yaw angles can be described as rotational angles around *x*-, *y*-, and *z*-axes of the insole in a world frame.

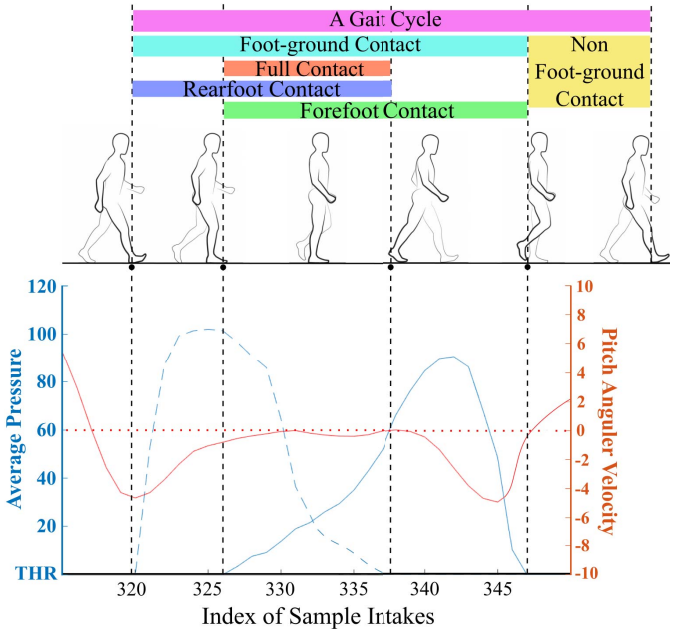

Fig. 4. Blue solid/dashed graph: the forefoot/rearfoot average pressure trend of a healthy subject extracted by SITUG during a gait cycle. Red solid graph: the pitch angular velocity of the subject in the gait cycle. Spatial–temporal features including forefoot contact, rearfoot contact, full contact, foot-ground contact, and foot-ground noncontact times are marked regarding the average pressure trends. All these features and their relationships with the average pressures are described in Table II.

the precise version under a 100 Hz sampling frequency [25], which is also the default sampling rate of Smart Insole.

Spatial features define the orientation of feet which plays an essential role in stride length calculation and TUG phase recognition. Additionally, the normality of gait can be assessed by checking patterns of three rotational angles, because a healthy subject usually performs similar pitch, roll, and yaw angle patterns during gait. The red colored graph in Fig. 4 is the pitch angular velocity trend of a healthy subject extracted by SITUG during a gait cycle.

C. Gait Feature Extraction: Spatial–Temporal Feature

All foot-ground contact related spatial–temporal features are determined by different average pressures [see Table II (1–6)]. During a foot-ground contact, solid forces are applied onto the ground such that sensors' inner structures are squeezed, producing noticeable pressure values. Fig. 4 presents the forefoot

TABLE II
DESCRIPTIONS AND METHODOLOGIES OF SPATIAL–TEMPORAL FEATURES

Features	Description	Methodology
0. Threshold (THR)	10% of the participant's sole avg. pressure in a natural standing posture.	Each participant stands for 10 seconds before the TUG process for finalizing THR.
1. Forefoot Contact Time	A period of forefoot in contact with the ground in a gait cycle.	The covered time of a collected time stamp set with the forefoot avg. pressure $\geq$ THR.
2. Rearfoot Contact Time	A period of rearfoot in contact with the ground in a gait cycle.	The covered time of a collected time stamp set with the rearfoot avg. pressure $\geq$ THR.
3. Full Contact Time	A period of entire foot in contact with the ground in a gait cycle.	The covered time of the intersection of time stamp sets collected from 1 and 2.
4. Foot-ground Contact Time	A period of foot in contact with the ground in a gait cycle.	The covered time of the union of time stamp sets collected from 1 and 2.
5. Non Foot-ground Contact Time	A period of foot completely in the air in a gait cycle.	The covered time of a collected time stamp set with every sensor's value $<$ THR.
6. Initial Contact Moment	The start of a latter gait cycle and the end of a former gait cycle.	The first time stamp within the union (aforementioned in 4).
7. Gait Cycle Time	The duration of a gait cycle.	The duration between two consecutive initial contact moments of one foot.
8. TUG Time	The duration of a TUG.	The time difference between the start and the end of TUG (see in Section. IV-D).
9. Gait Cycle Count	The number of performed gait cycles in a TUG.	The number of appeared non foot-ground contacts.
10. Gait Cycle Pace	The gait cycle count in one minute (60 seconds).	Gait cycle count divided by TUG time in seconds, and then times 60.
11. Stride Length	The horizontal displacement of a foot made in a gait cycle.	The algorithm is described in the second paragraph of Sec. IV-C and Fig. 5.

and the rearfoot average pressure trends corresponding to different foot-ground contacts in a normal gait cycle. Insoles may sense minor pressures without any foot-ground contact since they still contact with feet and shoes. Therefore, a threshold (THR) of the forefoot, the rearfoot, and the sole average pressures is used for determining foot-ground contact related spatial–temporal features. Instructed by SITUG, each subject stands for 10 s before the TUG process for finalizing THR [see Table II (0)], which is 10% of the subject's sole average pressure in a natural standing position.

The algorithm of stride length estimation, inspired by Laudanski *et al.* [26], uses processed data with drift and bias controls as mentioned in Section III-D. First, *x*-, *y*-, and *z*-axes linear accelerations from one sample intake are converted into an overall horizontal acceleration in the world frame using spatial features and trigonometric functions (see Fig. 5). A series of horizontal accelerations is then integrated into instantaneous horizontal velocities. In [26], an initial horizontal velocity of foot is added at the end of integration. However, SITUG considers the initial horizontal velocity as zero, since the algorithm is applied starting from a full contact in each gait cycle such that the foot is temporally stationary on the ground. Finally, we integrate the derived instantaneous velocities obtaining the horizontal displacement in each gait cycle, which is the stride length.

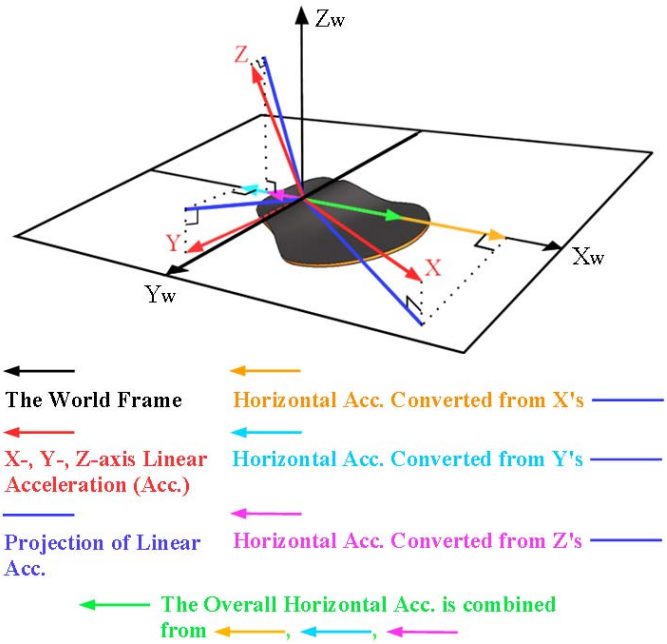

Fig. 5. In the world frame, an overall horizontal acceleration (green vector) is a combination of three horizontal accelerations (orange, cyan, and purple vectors), which are converted from blue projections of *x*-, *y*-, and *z*-axes linear accelerations (red vectors). Each projection is derived using spatial features (pitch, roll, and yaw angles) and trigonometric functions.

D. TUG Phase Recognition

Further information including the time taken to turn, which is highly useful in fall risk measurement [7], can be derived by the TUG phase recognition. Five consecutive TUG phases, including *lifting* (rising from a chair), *first walk* (walk to the turning point), *turning* (turn at the point), *second walk* (walk back to the chair), and *lowering* (sitting back down) are indicated by *six important time stamps*. The methodologies of locating these time stamps are described as follows.

1) Start of TUG: This time stamp is also the indicator of lifting phase. The plantar pressure increases since the start of TUG, the moment of starting to press feet onto the ground and trying to get up from the chair. The same THR [see Table II (0)] is used for determining the start of TUG as insoles sense minor plantar pressures while the subject is sitting with the feet on ground (a ready posture of TUG). For the first time, if both feet's sole average pressures exceed THR, then the start of TUG is stamped.

2) Start of First Walk: It is inevitable that each individual needs to lift a foot from the ground in order to step forward. While the foot is in non foot-ground contact time, the insole senses only minor pressures. Thus, for the first time when a sole average pressure of either left or right foot suddenly drops below the aforementioned THR [see Table II (0)], the start of first walk is located.

3) Start of Turning: The yaw angle difference D is equal to $|(\phi)_{\text{latter}} - (\phi)_{\text{former}}|$, where $(\phi)_{\text{latter}}$ represents a yaw angle upon a latter full contact and $(\phi)_{\text{former}}$ is the one upon a former full contact. In [27], D is defined as the turning angle such that an individual is in turning period when $D > 20°$. Their experimental walking procedure involves a smooth turn which would not produce sharp changes in D. In the setting of TUG, a sharp full turn is required leading to abrupt changes in D. Therefore, we empirically increase the THR to 75° for distinguishing the full turn from other mild, smooth turns occurring in Bypass TUG (see Section II-C). The start of turning is the

start of $D \geq 75°$, which must be consecutively satisfied by both feet.

4) Start of Second Walk: This time stamp is the first initial contact moment [defined in Table II (6)], which is the start of a gait cycle occurs immediately after the end of the turning phase such that the 75° requirement is no longer consecutively satisfied by both feet.

5) Start of Lowering: When the sitting down process begins, each individual tends to fix both feet on the ground and shift the body weight backward putting more pressures on heels. Thus, after the start of second walk, the start of lowering can be determined if the following three conditions are satisfied: 1) both feet's x-axis linear accelerations stay near zero; 2) the derivative of forefoot average pressure is negative; and 3) the derivative of rearfoot average pressure is positive.

6) End of TUG: This time stamp is also the end of lowering phase such that the subject is back to a natural sitting posture after the TUG process. Behind the start of lowering, if both feet's sole average pressures drop and stay less than the aforementioned THR in Section IV-D1, the TUG has ended.

V. Evaluation

A. Experimental Setup

Ten participants (age: 19 – 44; weight: 50 – 85 kg; height: 160 – 186 cm; body mass index: 18.4 – 27.1; shoe size: 37 – 44 in European standard; all have normal mobility; five females) volunteered for this experiment. Each participant completed a series of four environment-adapting TUGs; the used obstacles are all in the size of 42.2 cm (L) × 25.4 cm (W) × 18.8 cm (H). The data set was collected by the Smart Insole placed in the participant's shoes with 100 Hz as the sampling frequency and 12-bit as the resolution. Video filming was used with the purpose of setting ground truth references. We aimed at validating the feasibility of SITUG in monitoring movements within four environment-adapting TUGs designed to examine an individual's gait adaptability eliciting further information for fall risk assessment (see Section II-C).

B. Quantified Study

This paper verifies the accuracy of spatial–temporal features and TUG phase recognition proofing the feasibility of SITUG. A corresponding equation of accuracy (ACC) is

$$\mathrm{ACC} = \left(1 - \frac{|V_m - V_t|}{V_t}\right) \times 100\% \tag{1}$$

where V_m and V_t stand for the measured and the true values. In order to show the dispersion of calculated accuracies, standard deviations (SDs) are also computed as follows:

$$\mathrm{SD} = \sqrt{\frac{1}{N} \times \sum_{i=1}^{N} (x_i - \mu)^2} \tag{2}$$

where N is the amount of involved values, x_i is each individual value, and μ is the mean of all involved values. In statistics, it is well known that 68.3%, 95.5%, and 99.7% of involved values lie within the range of $\mu \pm \mathrm{SD}$, $\mu \pm 2\mathrm{SD}$, and $\mu \pm 3\mathrm{SD}$.

TABLE III
Experimental Results of Contact Related Features

Feature	Extended TUG	Incline TUG	Bypass TUG	Overpass TUG
	ACC(%): Mean±SD	ACC(%): Mean±SD	ACC(%): Mean±SD	ACC(%): Mean±SD
Forefoot Contact Time	94.23 ± 2.38	95.33 ± 2.81	92.95 ± 2.39	92.84 ± 2.47
Rearfoot Contact Time	94.17 ± 2.01	93.74 ± 2.12	93.80 ± 2.48	93.12 ± 2.50
Full Contact Time	93.62 ± 1.99	93.88 ± 2.22	94.37 ± 2.55	92.23 ± 2.07
Non Foot-ground Contact Time	94.34 ± 2.11	95.01 ± 2.63	93.87 ± 1.96	93.22 ± 1.88
Gait Cycle Time	94.81 ± 2.77	94.28 ± 2.34	94.60 ± 2.46	93.92 ± 2.08

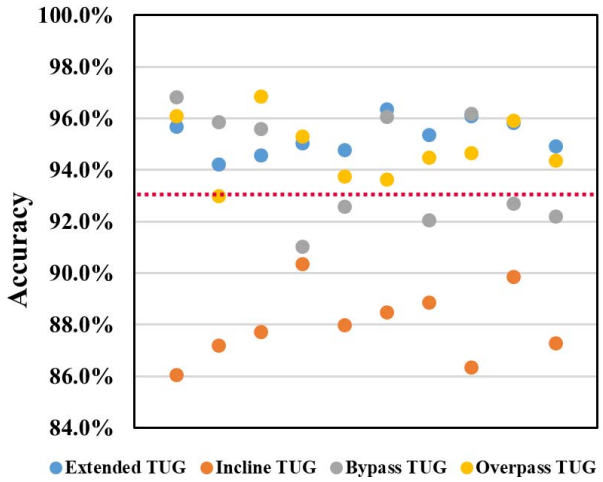

Fig. 6. Experimental results for stride length. Each circle is a calculated accuracy of WD of a TUG. The red dashed line indicates the mean of all accuracies. Four colors are used to distinguish types of TUG.

1) Contact Related Features: Multiple gait cycles are involved in a TUG. Therefore, for each TUG, mean forefoot, rearfoot, full, non foot-ground contact, and gait cycle times are computed. Comparing the computed mean times from SITUG's results and video observations, we obtain each contact related feature's accuracy in a TUG. For each type of TUG, ten accuracies of each contact related feature are calculated since each of ten subjects performs all types of environment-adapting TUG. The mean and the SD of every ten accuracies are presented in Table III. To clarify, validation results of gait cycle time assess SITUG's ability in locating initial contact moments, which directly determines the gait cycle time as described in Table II (7). Additionally, the correctness of extracted foot-ground contacts is already verified by the presented accuracies as forefoot, rearfoot, and full contacts are components of the foot-ground contact. According to the experimental results, SITUG achieves decent accuracies in all contact related features. We believe that this is due to the virtue of pressure sensors array as foot-ground contacts directly and significantly change the pressure of related plantar areas.

2) Gait Cycle Count and Stride Length: SITUG is reliable in counting gait cycles. In all performed TUGs, all accuracies of gait cycle count achieve 100%.

To access SITUG's capability in stride length estimation, we first derive the WD based on the estimated stride lengths. The equation of WD is

$$\mathrm{WD} = \frac{S_{\mathrm{left}} + S_{\mathrm{right}}}{2} \tag{3}$$

where S_{left} (S_{right}) is the sum of left (right) foot's all stride lengths performed in a TUG. The reference WD of extended,

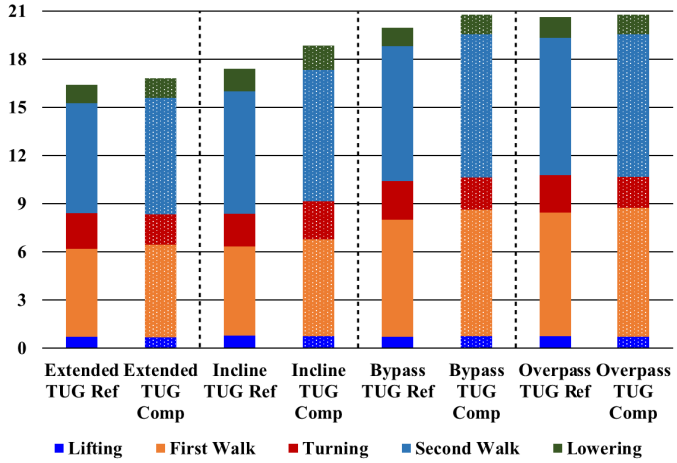

Fig. 7. Experimental results for TUG phase recognition. Each colored segment inside a column represents an average value of all duration of the corresponding TUG phase created by ten subjects. White dotted columns are computed results from SITUG while normal colored ones are reference values from video observations.

incline, and overpass TUGs is 14 m. For bypass TUG, the reference WD is 15.5 m. Comparing an estimated WD and the corresponding reference, an accuracy of stride length in each performed TUG is obtained. Fig. 6 shows our experimental results. The mean accuracy of stride length derived from WD validation is 93.06% (marked by a red dashed line in the figure).

We notice that the accuracy of stride length in incline TUG is always lower than the results of other environmental TUGs. This can be caused by the fixed world frame setting in SITUG. According to our current experimental setup, the world frame is initialized on the flat ground since it is defined at the start of each test. Therefore, when an individual is walking on an incline, the fixed world frame cannot finely match with the reality; the level of incompatibility is related to the degree of incline. Considering the advantages (e.g., data consistency and computing efficiency) of having a fixed world frame, one feasible solution is to start the incline TUG on the slope instead of the flat ground.

3) TUG Phase Recognition: For a phase in a type of TUGs, an average duration is taken from ten participants' phase durations recorded by SITUG or video filming. To assess the correctness of recognizing TUG phases, we check the inferred average duration of each phase in four different TUGs with reference values derived from video observations (see Fig. 7). Five mean accuracies are calculated for five extracted average TUG phase durations of all types of TUG, which are 95.38%, 93.80%, 83.44%, 94.40%, and 94.13%.

According to the experimental results, SITUG is more accurate in locating other TUG phases instead of the turning. Turns performed by different individuals can be greatly varied. Therefore, unlike other important time stamps (see Section IV-D), it is much difficult to define a standard start of turning from visualization (i.e., video filming) leading to deviations in turning phase recognition. The problem can be mitigated by informing participants a unified way of turning.

VI. Conclusion

Due to the existing drawbacks in TUG, we propose the SITUG designed for extracting rich and fine features in the environment-adapting TUGs, which advances current clinical standards for identifying individuals at risk for falling. SITUG consists of a sensor-equipped wearable device, a user-friendly smartphone application, and a well-considered cloud service module. It offers comprehensive gait feature extractions and distinguishes five detailed TUG phases, providing fine-grained information for fall risk estimation. According to the experimental results, SITUG can educe all contact related spatial–temporal features with all mean accuracies above 92% and recognize all TUG phases with a mean accuracy 92.23%. It is also competent in counting gait cycles achieving a 100% accuracy for all environmental-adapting TUGs. Moreover, it can estimate the WD with a mean accuracy 93.06% for verifying the stride length.

In the future, we plan to deploy a more rigorous version of experiment. First, we will evaluate the system in an older population. Second, we hope to validate SITUG using state-of-the-art equipments such as a motion capture camera system and a force platform. Afterwards, we believe that our system can be evolved to a next level of usability and reliability based on a finer experimental feedback.

Acknowledgment

The authors would like to thank the technical team of SennoTech Inc., Shenzhen, China, for discussions and facility supports.

References

[1] (2016). *Administration on Aging, Aging Statistics*. [Online]. Available: http://www.aoa.acl.gov/aging_statistics/index.aspx

[2] *National Council on Aging, Falls Prevention Facts*. Accessed: Apr. 15, 2018. [Online]. Available: https://www.ncoa.org/news/resources-for-reporters/get-the-facts/falls-prevention-facts/

[3] A. G. Society and B. G. Society, "Summary of the Updated American Geriatrics Society/British Geriatrics Society clinical practice guideline for prevention of falls in older persons," *J. Amer. Geriatrics Soc.*, vol. 59, pp. 150–151, Jan. 2011.

[4] E. Barry, R. Galvin, C. Keogh, F. Horgan, and T. Fahey, "Is the timed up and go test a useful predictor of risk of falls in community dwelling older adults: A systematic review and meta-analysis," *BMC Geriatrics*, vol. 14, no. 1, p. 14, 2014, doi: 10.1186/1471-2318-14-14.

[5] D. Schoene *et al.*, "Discriminative ability and predictive validity of the timed up and go test in identifying older people who fall: Systematic review and meta-analysis," *J. Amer. Geriatrics Soc.*, vol. 61, no. 2, pp. 202–208, 2013, doi: 10.1111/jgs.12106.

[6] E. Nordin, N. Lindelöf, E. Rosendahl, J. Jensen, and L. Lundin-Olsson, "Prognostic validity of the timed up-and-go test, a modified get-up-and-go test, staff's global judgement and fall history in evaluating fall risk in residential care facilities," *Age Ageing*, vol. 37, no. 4, pp. 442–448, 2008.

[7] G. Sprint, D. J. Cook, and D. L. Weeks, "Toward automating clinical assessments: A survey of the timed up and go," *IEEE Rev. Biomed. Eng.*, vol. 8, pp. 64–77, 2015.

[8] A. Salarian *et al.*, "iTUG, a sensitive and reliable measure of mobility," *IEEE Trans. Neural Syst. Rehabil. Eng.*, vol. 18, no. 3, pp. 303–310, Jun. 2010.

[9] *Kinesis QTUG Key Features*. Accessed: Apr. 15, 2018. [Online]. Available: http://www.kinesis.ie/qtug/

[10] L. Hak *et al.*, "Stepping strategies for regulating gait adaptability and stability," *J. Biomech.*, vol. 46, no. 5, pp. 905–911, Mar. 2013.

[11] V. Weerdesteyn, B. Nienhuis, and J. Duysens, "Advancing age progressively affects obstacle avoidance skills in the elderly," *Human Movement Sci.*, vol. 24, no. 5, pp. 865–880, 2005. [Online]. Available: http://www.sciencedirect.com/science/article/pii/S0167945705000898
[12] M. D. J. Caetano, "Sensorimotor and cognitive predictors of impaired gait adaptability in older people," *J. Gerontol.*, vol. 72, no. 9, pp. 1257–1263, Sep. 2017.
[13] R. A. Ferraro, G. Pinto-Zipp, S. Simpkins, and M. Clark, "Effects of an inclined walking surface and balance abilities on spatiotemporal gait parameters of older adults," *J. Geriatric Phys. Therapy*, vol. 36, no. 1, pp. 31–38, 2013.
[14] Z. Yang, C. Song, F. Lin, J. Langan, and W. Xu, "Empowering a gait feature-rich timed-up-and-go system for complex ecological environments," in *Proc. IEEE/ACM Int. Conf. Connected Health Appl. Syst. Eng. Technol. (CHASE)*, Philadelphia, PA, USA, Jul. 2017, pp. 340–347.
[15] D. Berrada, M. Romero, G. Abowd, M. Blount, and J. Davis, "Automatic administration of the get up and go test," in *Proc. 1st ACM SIGMOBILE Int. Workshop Syst. Netw. Support Healthcare Assisted Living Environ.*, Jun. 2007, pp. 73–75.
[16] F. Wang, M. Skubic, C. Abbott, and J. M. Keller, "Quantitative analysis of 180 degree turns for fall risk assessment using video sensors," in *Proc. Int. Conf. IEEE Eng. Med. Biol. Soc. Annu. (EMBC)*, Dec. 2011, pp. 7606–7609.
[17] L. Z. Rubenstein and K. R. Josephson, "Falls and their prevention in elderly people: What does the evidence show?" *Med. Clinics North America*, vol. 90, no. 5, pp. 807–824, Sep. 2006.
[18] M. F. Vieira *et al.*, "Gait stability, variability and complexity on inclined surfaces," *J. Biomech.*, vol. 54, pp. 73–79, Mar. 2017.
[19] M. J. D. Caetano *et al.*, "Age-related changes in gait adaptability in response to unpredictable obstacles and stepping targets," *Gait Posture*, vol. 46, pp. 35–41, May 2016.
[20] F. Lin, A. Wang, L. Cavuoto, and W. Xu, "Toward unobtrusive patient handling activity recognition for injury reduction among at-risk caregivers," *IEEE J. Biomed. Health Inform.*, vol. 21, no. 3, pp. 682–695, May 2017.
[21] A. R. Anwary, H. Yu, and M. Vassallo, "Optimal foot location for placing wearable IMU sensors and automatic feature extraction for gait analysis," *IEEE Sensors J.*, vol. 18, no. 6, pp. 2555–2567, Mar. 2018.
[22] E. B. Titianova, P. S. Mateev, and I. M. Tarkka, "Footprint analysis of gait using a pressure sensor system," *J. Electromyography Kinesiol.*, vol. 14, no. 2, pp. 275–281, 2004. [Online]. Available: http://www.sciencedirect.com/science/article/pii/S1050641103000774
[23] B. Mariani, H. Rouhani, X. Crevoisier, and K. Aminian, "Quantitative estimation of foot-flat and stance phase of gait using foot-worn inertial sensors," *Gait Posture*, vol. 37, no. 2, pp. 229–234, Feb. 2013.
[24] V. Lugade and K. Kaufman, "Center of pressure trajectory during gait: A comparison of four foot positions," *Gait Posture*, vol. 40, no. 1, pp. 252–254, May 2014.
[25] A. Janota, V. Šimák, D. Nemec, and J. Hrbček, "Improving the precision and speed of euler angles computation from low-cost rotation sensor data," *Sensors*, vol. 15, no. 3, pp. 7016–7039, Mar. 2015.
[26] A. Laudanski, S. Yang, and Q. Li, "A concurrent comparison of inertia sensor-based walking speed estimation methods," in *Proc. Annu. Int. Conf. IEEE Eng. Med. Biol. Soc.*, Aug. 2011, pp. 3484–3487.
[27] B. Mariani *et al.*, "3D gait assessment in young and elderly subjects using foot-worn inertial sensors," *J. Biomech.*, vol. 43, no. 15, pp. 2999–3006, Nov. 2010.

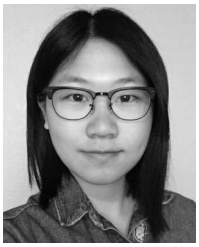

Zhuolin Yang (S'18) is currently pursuing the undergraduation degree at the Computer Science and Engineering Department, State University of New York at Buffalo, Buffalo, NY, USA.

She is with the Embedded Sensing and Computing Laboratory, State University of New York at Buffalo, as a Research Assistant, under the direction of Prof. W. Xu. Her current research interests include pervasive health, embedding sensors systems, and mobile computing.

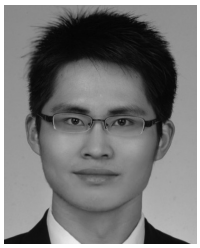

Chen Song (S'14) received the B.S. degree in optic science and engineering from Fudan University, Shanghai, China, and the M.S. degree in electrical engineering from the State University of New York at Buffalo, Buffalo, NY, USA, where he is currently pursuing the Ph.D. degree at the Department of Computer Science under the direction of Prof. W. Xu.

His current research interests include mobile smart health, cyber physical security, and emerging biometrics.

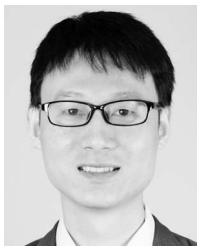

Feng Lin (S'11–M'15) received the B.S. degree from Zhejiang University, Hangzhou, China, the M.S. degree from Shanghai University, Shanghai, China, and the Ph.D. degree from the Department of Electrical and Computer Engineering, Tennessee Technological University, Cookeville, TN, USA.

He is currently an Assistant Professor with the Department of Computer Science and Engineering, University of Colorado Denver, Denver, CO, USA. He was a Research Scientist with the State University of New York at Buffalo, Buffalo, NY, USA, and performed research with Alcatel-Lucent (currently Nokia), Boulogne-Billancourt, France. His current research interests include mobile sensing, healthcare IoT, and cyber-physical security.

Dr. Lin was a recipient of the First Prize Design Award of the 2016 International 3-D Printing Competition, Best Paper Award of the IEEE BHI Conference, and the Best Demo Award of the ACM HotMobile Conference.

Jeanne Langan (M'06) received the B.A. degree in physical therapy in 1990, the M.S. degree in exercise and movement science in 2002, and the Ph.D. degree in human physiology in 2006.

She is currently an Assistant Professor with the Department of Rehabilitation Science, University at Buffalo, Buffalo, NY, USA. Her current research interests include developing portable rehabilitation systems capable of providing users feedback on motor performance. These rehabilitation systems are designed to support recovery across the lifespan of individuals with chronic motor deficits.

Wenyao Xu (M'13) received the B.S. and M.S. degrees (Hons.) from Zhejiang University, Hangzhou, China, in 2006 and 2008, respectively, and the Ph.D. degree from the University of California at Los Angeles, Los Angeles, CA, USA, in 2013.

He is currently an Associate Professor with the Computer Science and Engineering Department, State University of New York at Buffalo, Buffalo, NY, USA. He has intensively collaborated with many industrial companies in the past years. He has authored or co-authored over 130 research papers, co-authored 2 books, and has been named as an inventor on 6 international and U.S. patents. His current research interests include smart health, Internet of Things, and emerging biometrics.

Dr. Xu was a recipient of six Best Paper Awards. He has served on the Technical Program Committee of numerous international conferences in the field of smart health, mobile computing, and Internet of Things, and has been the TPC Co-Chair of IEEE BSN 2018.